JOC Article

Expanding the Registry of Aromatic Amide Foldamers: Folding, Photochemistry and Assembly Using Diaza-anthracene Units

Emanuela Berni,[†] Christel Dolain,[†] Brice Kauffmann,[§] Jean-Michel Léger,[‡] Chuanlang Zhan,[†] and Ivan Huc[†,*]

Université Bordeaux 1−CNRS UMR 5248, Institut Européen de Chimie et Biologie, 2 rue Robert Escarpit, 33607 Pessac Cedex, France, Université Bordeaux 1−Université Victor Segalen Bordeaux 2−CNRS UMS 3033, Institut Européen de Chimie et Biologie, 2 rue Robert Escarpit, 33607 Pessac Cedex, France, and Laboratoire de Pharmacochimie, Université Victor Segalen Bordeaux 2, 146 rue Léo Saignat, 33076 Bordeaux, France

i.huc@iecb.u-bordeaux.fr

Received December 6, 2007

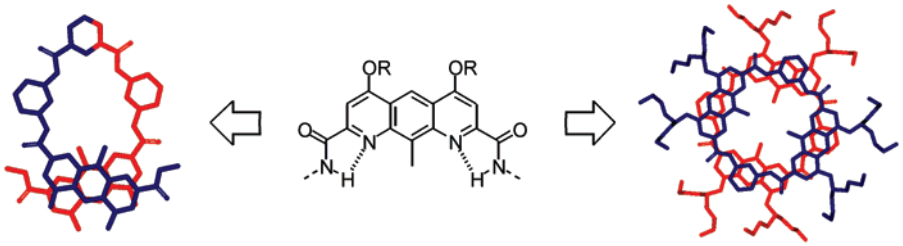

The synthesis of various 1,8-diaza-4,5-dialkoxy-2,7-anthracene dicarboxylic acid derivatives and their incorporation into cyclic and helically folded aromatic oligoamides are reported. The ability of the diaza-anthracene monomers to undergo photoaddition or head-to-tail photodimerization was investigated in the solid state and in solution. Quantitative conversion of a monomer diester to the corresponding head-to-tail photodimer could be achieved in the solid state without protection from oxygen. The formation of an emissive excimer between two diaza-anthracene units appended at the end of a helically folded oligomer was demonstrated. Intramolecular photodimerization was not observed in this compound, possibly due to the low thermal stability of the head-to-head photoadduct. A cyclic oligoamide composed of two diaza-anthracene and two pyridine units was shown to adopt a flat conformation and to form columnar stacks in the solid state. Longer, noncyclic oligoamides composed of one or two diaza-anthracene units were shown to adopt helical conformations that exist preferentially as double helical dimers.

Introduction

Secondary aromatic amide foldamers have demonstrated high potential for adopting well-defined helical or linear conformations inspired from the secondary structures of biopolymers.[1] When hydrogen bond donors or acceptors are introduced on an aryl ring in a position adjacent to an amide function, a preferred conformation occurs at the aryl-amide linkage as a result of conjugation, intramolecular hydrogen bonding with the amide CO or NH moieties, and electrostatic interactions. Upon applying this concept to an entire aryl amide sequence, a wide range of stable folded states can be reached that represent a linear combination of the local conformational preferences and that may be further stabilized by intramolecular aromatic stacking as, for example, in helical conformations.

The high predictability, tunability, and conformational stability of these folded architectures, as well as their resistance to chemical and biochemical hydrolysis, make them particularly attractive as scaffolds for a wide range of applications in biological and material sciences. For instance, some linear oligomers display antibiotic properties[2] and have been used as

[†] Université Bordeaux 1−CNRS UMR 5248.
[§] Université Bordeaux 1−Université Victor Segalen Bordeaux 2−CNRS UMS 3033.
[‡] Laboratoire de Pharmacochimie, Université Victor Segalen Bordeaux 2.

(1) For reviews, see: Cuccia, L.; Huc, I. Foldamers Based on Local Conformational Preferences. In *Foldamers: Structure, Properties and Applications*; Hecht, S., Huc, I., Eds.; Wiley-VCH: Weinheim, 2007; pp 3−33. Li, Z.-T.; Hou, J.-L.; Li, C.; Yi, H.-P. *Chem.− Asian J.* **2006**, *1*, 766. Huc, I. *Eur. J. Org. Chem.* **2004**, 17. Gong, B. *Chem. Eur. J.* **2001**, *7*, 4336.

(2) Tew, G. N.; Liu, D. H.; Chen, B.; Doerksen, R. J.; Kaplan, J.; Carroll, P. J.; Klein, M. L.; DeGrado, W. F. *Proc. Natl. Acad. Sci. U.S.A.* **2002**, *99*, 5110.

10.1021/jo702602w CCC: $40.75
Published on Web 03/11/2008

mimics of α-helices[3] and to recognize heparin.[4] Some helical oligomers readily cross cell membranes,[5] have high affinity for G-quadruplex DNA,[6] and show great potential for the molecular recognition of guests as diverse as fullerenes,[7] sugars,[8] or small polar molecules.[9] A recent example of a very large (>8 kDa) aromatic amide folded architecture hints at the possibility to elaborate functional objects as complex as proteins based on aromatic backbones.[10] Additionally, the ability of some of these oligomers to form well-defined assemblies such as double helical hybrids[11] or hydrogen-bonded tapes[12] further extends the analogy with the folding and assembling properties of biomolecules and has been used to selectively template chemical reactions.[13]

As in α-peptides and their β and γ homologues,[14] the properties and functions of aromatic amide foldamers greatly depend upon the nature of the side chains introduced in the sequence. In addition, the nature of the aromatic rings that constitute the main chain makes it possible to finely tune the folded architectures,[1] e.g., linear versus bent, helical with a small or a large diameter, and thus the orientation of the side chains. Among the factors that determine strand curvature are (i) the relative orientation of the amide functions on the aryl group; (ii) the number of rings of the aromatic group; and (iii) the pinching of the strand through five-membered or six-membered intramolecular hydrogen-bonded rings.

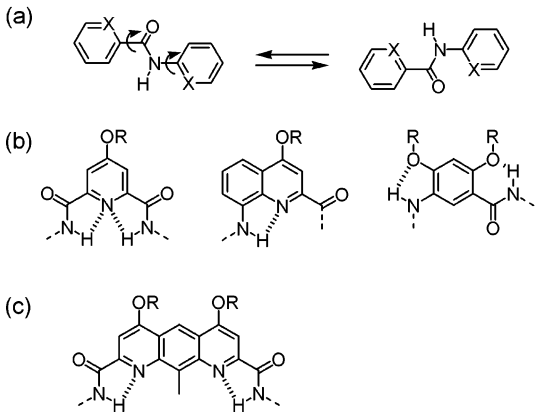

FIGURE 1. (a) Local rotational restrictions of aryl amide bonds. Conformational preferences vary according to the nature of X. (b) Common aromatic amide foldamer building blocks. (c) 1,8-Diaza-anthracene unit studied in this report.

Expanding the registry of available building blocks for aromatic amide foldamer design is thus an important task to widen the scope of their applications. Common building blocks of aromatic amide foldamers include pyridines and pyridiniums,[9,11,15,16] quinolines[5,6,9,10,17] anthranilic acids,[16] pyridine oxides,[11e,16a] alkoxybenzenes,[7,8,12,13,16,18] pyrazines,[19] and fluorobenzenes (Figure 1).[20] Here, we report on aromatic amide foldamers composed of pyridine rings and 1,8-diaza-2,7-anthracenedicarboxamide units.[21] When inserted in an oligoamide sequence, these units are expected to behave as an expanded 2,6-pyridinedicarboxamide monomer: aryl-amide

(3) Ernst, J. T.; Becerril, J.; Park, H. S.; Yin, H.; Hamilton, A. D. *Angew. Chem., Int. Ed.* **2003**, *42*, 535.

(4) Choi, S.; Clements, D. J.; Pophristic, V.; Ivanov, I.; Vemperala, S.; Bennett, J. S.; Klein, M. L.; Winkler, J. D.; DeGrado, W. F. *Angew. Chem., Int. Ed.* **2005**, *44*, 6685.

(5) Gillies, E. R.; Deiss, F.; Staedel, C.; Schmitter, J.-M.; Huc, I. *Angew. Chem., Int. Ed.* **2007**, *46*, 4081.

(6) Shirude, P. S.; Gillies, E. R.; Ladame, S.; Godde, F.; Shin-ya, K.; Huc, I.; Balasubramanian, S. *J. Am. Chem. Soc.* **2007**, *129*, 11890.

(7) Wu, Z.-Q.; Shao, X.-B.; Li, C.; Hou, J.-L.; Wang, K.; Jiang, X.-K.; Li, Z.-T. *J. Am. Chem. Soc.* **2005**, *127*, 17460.

(8) (a) Li, C.; Wang, G. T.; Y, H. P.; Jiang, X. K.; Li, Z. T.; Wang, R. X. *Org. Lett.* **2007**, *9*, 1797. (b) Hou, J.-L.; Shao, X.-B.; Chen, G.-J.; Zhou, Y.-X.; Jiang, X.-K.; Li, Z.-T. *J. Am. Chem. Soc.* **2004**, *126*, 12386. (c) Hou, J.-L.; Jia, M.-X.; Jiang, X.-K.; Li, Z.-T.; Chen, G.-J. *J. Org. Chem.* **2004**, *69*, 6228.

(9) (a) Garric, J.; Léger, J.-M.; Huc, I. *Angew. Chem., Int. Ed.* **2005**, *44*, 1954. (b) Garric, J.; Léger, J.-M.; Huc, I. *Chem. Eur. J.* **2007**, *13*, 8454.

(10) Delsuc, N.; Léger, J.-M.; Massip, S.; Huc, I. *Angew. Chem., Int. Ed.* **2007**, *46*, 214.

(11) (a) Berl, V.; Huc, I.; Khoury, R. G.; Krische, M. J.; Lehn, J.-M.; Schmutz, R. *Nature* **2000**, *407*, 720. (b) Berl, V.; Huc, I.; Khoury, R. G.; Lehn, J.-M.; Schmutz, R. *Chem. Eur. J.* **2001**, *7*, 2810. (c) Jiang, H.; Maurizot, V.; Huc, I. *Tetrahedron* **2004**, *60*, 10029. (d) Acocella, A.; Venturini, A.; Zerbetto, F. J. *J. Am. Chem. Soc.* **2004**, *126*, 2362. (e) Dolain, C.; Zhan, C.; Léger, J.-M.; Huc, I. *J. Am. Chem. Soc.* **2005**, *127*, 2400. (f) Haldar, D.; Jiang, H.; Léger, J.-M.; Huc, I. *Angew. Chem., Int. Ed.* **2006**, *45*, 5483. (g) Zhan, C.; Léger, J.-M.; Huc, I. *Angew. Chem., Int. Ed.* **2006**, *45*, 4625. (h) Haldar, D.; Jiang, H.; Léger, J.-M.; Huc, I. *Tetrahedron* **2007**, *63*, 6322. (i) Berni, E.; Kauffmann, B.; Bao, C.; Lefeuvre, J.; Bassani, D. M.; Huc, I. *Chem. Eur. J.* **2007**, *13*, 8463.

(12) (a) Nowick, J. S.; Holmes, D. L.; Mackin, G.; Norhona, G.; Shaka, A. J.; Smith, E. M. *J. Am. Chem. Soc.* **1996**, *118*, 2764. (b) Nowick, J. S.; Pairish, M.; Queen Lee, I.; Holmes, D. L.; Ziller, J. W. *J. Am. Chem. Soc.* **1997**, *119*, 5413. (c) Nowick, J. S. *Acc. Chem. Res.* **1999**, *32*, 287. (d) Gong, B.; Yan, Y. F.; Zeng, H. Q.; Skrzypczak-Jankunn, E.; Kim, Y. W.; Zhu, J.; Ickes, H. *J. Am. Chem. Soc.* **1999**, *121*, 5607. (e) Zeng, H. Q.; Miller, R. S.; Flowers, R. A.; Gong, B. *J. Am. Chem. Soc.* **2000**, *122*, 2635. (f) Zhu, J.; Lin, J.-B.; Xu, Y.-X.; Shao, X.-B.; Jiang, X.-K.; Li, Z.-T. *J. Am. Chem. Soc.* **2006**, *128*, 12307.

(13) (a) Yang, X.; Gong, B. *Angew. Chem., Int. Ed.* **2005**, *44*, 1352. (b) Li, M.; Yamato, K.; Ferguson, J. S.; Gong, B. *J. Am. Chem. Soc.* **2006**, *128*, 12628.

(14) For a review, see: Le Grel, P.; Guichard G. Foldamers Based on Remote Intrastrans Interactions. In *Foldamers: Structure, Properties and Applications*; Hecht, S., Huc, I., Eds.; Wiley-VCH: Weinheim, 2007; pp 35−75.

(15) (a) Berl, V.; Huc, I.; Khoury, R. G.; Lehn, J.-M. *Chem. Eur. J.* **2001**, *7*, 2798. (b) Huc, I.; Maurizot, V.; Gornitzka, H.; Léger, J.-M. *Chem. Commun.* **2002**, 578. (c) Dolain, C.; Maurizot, V.; Huc, I. *Angew. Chem., Int. Ed.* **2003**, *42*, 2737. (d) Kolomiets, E.; Berl, V.; Odriozola, I.; Stadler, A.-M.; Kyritsakas, N.; Lehn, J.-M. *Chem. Commun.* **2003**, 2868.

(16) (a) Hamuro, Y.; Geib, S. J.; Hamilton, A. D. *J. Am. Chem. Soc.* **1997**, *119*, 10587. (b) Hamuro, Y.; Geib, S. J.; Hamilton, A. D. *J. Am. Chem. Soc.* **1996**, *118*, 7529.

(17) (a) Jiang, H.; Léger, J.-M.; Dolain, C.; Guionneau, P.; Huc, I. *Tetrahedron* **2003**, *59*, 8365. (b) Jiang, H.; Léger, J.-M.; Huc, I. *J. Am. Chem. Soc.* **2003**, *125*, 3448. (c) Maurizot, V.; Dolain, C.; Leydet, Y.; Léger, J.-M.; Guionneau, P.; Huc, I. *J. Am. Chem. Soc.* **2004**, *126*, 10049. (d) Jiang, H.; Dolain, C.; Léger, J.-M.; Gornitzka, H.; Huc. I. *J. Am. Chem. Soc.* **2004**, *126*, 1034. (e) Dolain, C.; Léger, J.-M.; Delsuc, N.; Gornitzka, H.; Huc, I. *Proc. Natl. Acad. Sci. U.S.A.* **2005**, *102*, 16146. (f) Dolain, C.; Jiang, H.; Léger, J.-M.; Guionneau, P.; Huc I. *J. Am. Chem. Soc.* **2005**, *127*, 12943. (g) Gillies, E. R.; Dolain, C.; Leger, J.-M.; Huc, I. *J. Org. Chem.* **2006**, *71*, 7931.

(18) (a) Zeng, H.; Ickes, H.; Flowers, R. A., II; Gong, B. *J. Org. Chem.* **2001**, *66*, 3574. (b) Zeng, H.; Yang, X.; Flowers, R. A., II; Gong, B. *J. Am. Chem. Soc.* **2002**, *124*, 2903. (c) Gong, B.; Zeng, H.; Zhu, J.; Yuan, L.; Han, Y.; Cheng, S.; Furukawa, M.; Parra, R. D.; Kovalevsky, A. Y.; Mills, J. L.; Skrzypczak-Jankun, E.; Martinovic, S.; Smith, R. D.; Zheng, C.; Szyperski, T.; Zeng, X. C. *Proc. Natl. Acad. Sci. U.S.A.* **2002**, *99*, 11583. (d) Yuan, L.; Sanford, A. R.; Feng, W.; Zhang, A.; Zhu, J.; Zeng, H.; Yamato, K.; Li, M.; Ferguson, J. S.; Gong, B. *J. Org. Chem.* **2005**, *70*, 10660. (e) Yuan, L.; Zeng, H.; Yamato, K.; Sanford, A. R.; Feng, W.; Atreya, H. S.; Sukumaran, D. K.; Szyperski, T.; Gong, B. *J. Am. Chem. Soc.* **2004**, *126*, 16528. (f) Zhu, J.; Lin, J.-B.; Xu, Y.-X.; Shao, X.-B.; Jiang, X.-K.; Li, Z.-T. *J. Am. Chem. Soc.* **2006**, *128*, 12307. (g) Hou, J. L.; Shao, X.-B.; Chen, G.-J.; Zhou, Y.-X.; Jiang, X.-K.; Li, Z.-T. *J. Am. Chem. Soc.* **2004**, *126*, 12386.

(19) Delnoye, D. A. P.; Sijbesma, R. P.; Vekemans, J. A. J. M.; Meijer, E. W. *J. Am. Chem. Soc.* **1996**, *118*, 8717.

(20) Li, C.; Ren, S.-F.; Hou, J.-L.; Yi, H.-P.; Zhu, S.-Z.; Jiang, X.-K.; Li, Z.-T. *Angew. Chem., Int. Ed.* **2005**, *44*, 5725.

(21) 1,8-Diaza-anthracenes are formally pyrido-quinolines, but their photochemical and photophysical behaviors relate to that of anthracene. These units were thus named diaza-anthracenes in this manuscript.

SCHEME 1. Synthesis of Monomers 2, 3a, 4a and Their Derivatives[a]

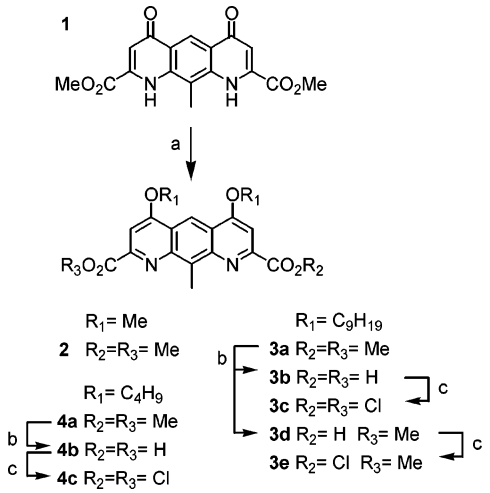

[a] Reagents and conditions: (a) MeI, K_2CO_3, DMF at 60 °C, 12 h, 44% yield or PPH_3, DIAD, ROH, THF, 12 h, 90% yield; (b) NaOH, dioxane/H_2O, 2 h, 50−100% yield; (c) $SOCl_2$, reflux or 1-chloro-*N*,*N*,2-trimethylpropenylamine, $CHCl_3$, 2 h, quantitative.

linkages should adopt *anti* conformations as a result of the endocyclic nitrogen atoms ortho to each carboxamide.

Anthracene-derived monomers are larger than the six-membered aromatic rings generally used in aromatic amide foldamers. They thus provide an extended surface expected to enhance intramolecular $\pi-\pi$ interactions and to help decrease oligomer curvature. Additionally their photochemical and photophysical properties may be exploited to elicit specific functions. In a previous report,[11i] we have shown that one such unit in the middle of a helically folded pyridine carboxamide sequence leads to the expected enlarged diameter and to a dramatic enhancement of the hybridization of the strand into a double helix. In this paper, we describe the folding and assembly of three oligomers with helical or macrocyclic structures that contain two 1,8-diaza-anthrancene moieties. We also report initial investigations of the photophysical and photochemical properties of the 1,8-diaza-anthracene units.

Results and Discussion

Synthesis. 1,8-Diaza-anthracene monomers were all derived from the pyridono-quinolone **1**. This compound is easily prepared in two steps from 2,6-diaminotoluene and dimethyl acetylene dicarboxylate using literature procedures.[22] Thus, each amine function of 2,6-diaminotoluene adds to an acetylene group to give an intermediate fumarate that is thermally cyclized into **1** in refluxing diphenyl ether. Diaminotoluene and not diaminobenzene was used to direct the cyclization step and avoid the formation of a phenanthrene derivative. The oxo functions in positions 4 and 5 of **1** were alkylated using MeI and K_2CO_3 in DMF to yield **2** or under Mitsunobu conditions using isobutanol or 5-nonanol to yield **4a** and **3a**, respectively (Scheme 1). As in pyridine[11,15] and quinoline[5,6,10,17] oligomers, the alkyl chains in positions 4 and 5 should diverge from the folded structures and determine their solubility and crystallinity. Three types of alkyl chains were tested, methyl, 5-nonyl, and isobutyl. All were found to be well compatible with single-crystal growth.

(22) Molock, F. F.; Boykin, D. W. *J. Heterocycl. Chem.*, **1983**, *20*, 681.

SCHEME 2. Synthesis of Pentamer 6[a]

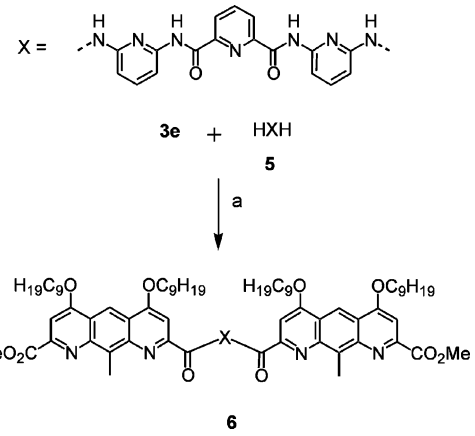

[a] Reagents and conditions: (a) Et_3N, THF, 16 h, 16% yield.

SCHEME 3. Synthesis of Macrocycle 7[a]

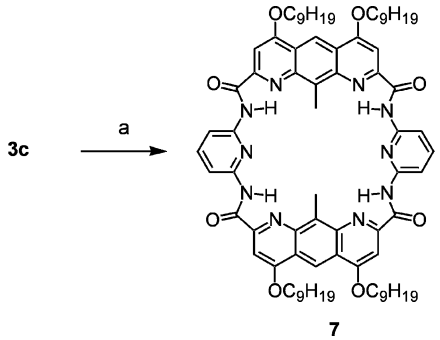

[a] Reagents and conditions: (a) 2,6-diaminopyridine, *i*PR_2NEt, THF, 16 h, 50% yield.

As could be expected, the methyl derivatives are all less soluble. The Mitsunobu reaction is a particularly efficient and versatile method to introduce the side chains. While the present work was performed in organic solvent, it could be transposed to water using polar side chain instead of alkyl chains.[5,6,17g]

Diesters **3a** and **4a** were saponified to the corresponding diacids **3b** and **4b**, which were converted to their acid chlorides **3c** and **4c** (Scheme 1). Diester **3a** was also disymmetrized into monoester monoacid **3d**, which was activated to the monoester mono acid chloride **3e**. Activations were initially performed with $SOCl_2$ but recent experiments involved milder conditions using 1-chloro-*N*,*N*,2-trimethylpropenylamine.[23] Coupling of the monoacid chloride **3e** with the two amine functions of trimeric pyridine oligomer **5**[15a] gave a pentameric sequence **6** with two terminal diaza-anthracene units (Scheme 2). When reacted with one equivalent of 2,6-diaminopyridine, diacid chloride **3c** gave macrocyclic tetramer **7** (Scheme 3). The yield was 50% even at a relatively high concentration (3.6 mM), illustrating the preferred bent conformation of the macrocycle precursors that favor the cyclization step. This yield is consistent with results reported for other so-called shape persistent macrocycles.[24] As reported previously,[11i] diacid chloride **4c** was coupled to the BOC-monoprotected diamino-pyridine trimer **8**[15a] to synthesize

(23) Ghosez, L.; Haveaux, B.; Viehe, H. G. *Angew. Chem., Int. Ed. Engl.* **1969**, *8*, 454.

(24) Jiang, H.; Léger, J.-M.; Guionneau, P.; Huc, I. *Org. Lett.* **2004**, *6*, 2985. Yuan, L.; Feng, W.; Yamato, K.; Sanford, A. R.; Xu, D.; Guo, H.; Gong, B. *J. Am. Chem. Soc.* **2004**, *126*, 11120. Xing, L.; Ziener, U.; Sutherland, T. C.; Cuccia, L. A. *Chem. Commun.* **2005**, *46*, 5751.

SCHEME 4. Synthesis of Heptamer 9 and Octamer 10[a]

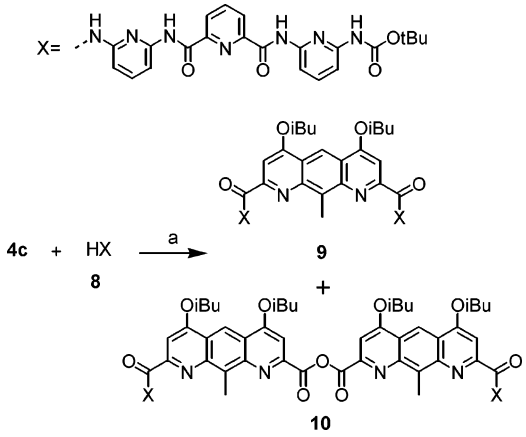

[a] Reagents and conditions: (a) *i*PR$_2$NEt, THF, 12 h, 66% yield (**9**) and 4% yield (**10**).

heptameric strand **9** (Scheme 4). During this reaction, octameric anhydride **10** was recurrently isolated as a side product in 4% yield. The formation of **10** was presumed to arise from the in situ hydrolysis of acid chloride functions due to residual water. However, attempts to improve this yield, for example, using stoichiometric amounts of **4c** and **8**, proved unsuccessful. Compound **10** nevertheless appeared to be worthy of studying (see below). As we have shown in quinoline oligomers, the anhydride function is fully compatible with the helical folding mode of aza-aromatic oligoamides.[17e] These anhydrides actually prove chemically very stable as they are isolated on silica gel chromatography taking no particular precaution, even in the presence of MeOH.

Photochemical Studies. Diester monomers **2**, **3a** and **4a** display UV absorption and emission spectra typical of anthracene derivatives (see below), suggesting that they possess comparable photophysical and photochemical properties. We were intrigued by the possibility to use the classical photodimerization of anthracenes within oligomers bearing several diaza-anthracene units. This reaction could indeed lead to the light-induced covalent capture of the helical foldamer into a helicene-like molecule, as has been achieved in other aromatic foldamers.[25]

Anthracene photodimerization under irradiation by visible light is one of the oldest known photochemical reactions.[26] The dimer is connected by two covalent bonds resulting from the [4 + 4] cycloaddition and reverts to anthracene thermally or with UV irradiation below 300 nm. The effects of substituents on the anthracene photodimerization in a head-to-tail (HT) or head-to-head (HH) conformation have been of longstanding interest and have been studied in detail,[27,28] even though studies of diaza-anthracene derivatives are scarce.[29] The reversible

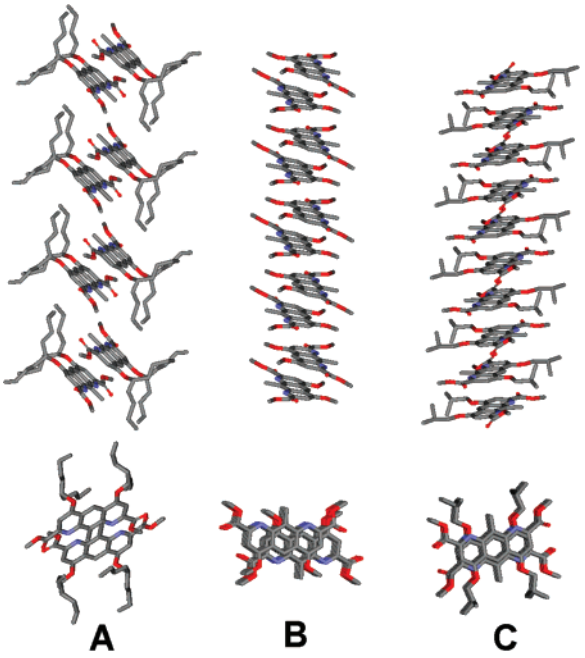

FIGURE 2. Columnar packing (top) and top views (bottom) of the solid-state structures of 1,8-diaza-anthracene monomers: (A) **3a**, crystallized from CH_2Cl_2/heptane; (B) **2** and (C) **4a**, both crystallized from nitrobenzene/acetonitrile. Hydrogen atoms and solvent molecules have been omitted for clarity.

dimerization and photochromic properties of poly and monosubstituted anthracene derivatives are at the basis of many potential applications, such as photoswitchable receptors.[30]

Prior to photochemical studies, crystallographic investigations were carried out on **2**, **3a**, and **4a**. The solid-state structure of all three compounds as anthracene monomers were characterized by X-ray diffraction of single crystals (Figure 2). All form columnar stacks where diaza-anthracene units engage in $\pi-\pi$ interactions, always in a HT orientation. The expected large dipole moment of these aromatic groups probably contributes to the stability of the HT arrangement. In the case of isobutyl derivative **4a**, each anthracene unit is exactly at the same distance of the anthracenes above and below along the stack, the nearest neighbor intermolecular C9−C10 distances all being 3.58 Å. In the structure of the methyl derivative **2**, diaza-anthracenes form HT pairs which are slightly offset from one another in the stack. Within a pair, the intermolecular C9−C10 distance is 3.58 Å, while between pairs it is 4.57 Å. In the structure of nonyl derivative **3a**, the pairs are fully individualized. Within a pair, the intermolecular C9−C10 distance is 3.78 Å; the second shortest intermolecular distance C9−C10 is above 8 Å.

Photodimerization studies were first carried out on **3a**. Upon prolonged irradiation of a large crystal of that compound under the intense visible light of a xenon-mercury lamp using a glass slide to cut off wavelengths below 300 nm, the bright yellow color faded away, suggesting an alteration of the anthracene chromophore, and the initially transparent crystal became opaque (Figure 3). X-ray measurements of the final solid showed a

(25) (a) Hecht, S.; Kan, A. *Angew. Chem., Int. Ed.* **2003**, *42*, 6021. (b) Masu, H.; Mizutani, I.; Kato, T.; Azumaya, I.; Yamaguchi, K.; Kishikawa, K.; Kohmoto, S. *J. Org. Chem.* **2006**, *71*, 8037.

(26) Becker, H. D. *Chem. Rev.* **1993**, *93*, 145.

(27) (a) Bouas-Laurent, H.; Castellan, A.; Desvergne, J.-P.; Lapouyade, R. *Chem. Soc. Rev.* **2000**, *29*, 43. (b) Bouas-Laurent, H.; Castellan, A.; Desvergne, J.-P.; Lapouyade, R. *Chem. Soc. Rev.* **2001**, *30*, 248.

(28) For recent examples, see: (a) Nakamura, A.; Inoue, Y. *J. Am. Chem. Soc.* **2005**, *127*, 5338. (b) Yang, C.; Nakamura, A.; Fukuhara, G.; Origane, Y.; Mori, T.; Wada, T.; Inoue, Y. *J. Org. Chem.* **2006**, *71*, 3126. Horiguchi, M.; Ito, Y. *J. Org. Chem.* **2006**, *71*, 3608.

(29) Jouvenot, D.; Glazer, E. C.; Tor, Y. *Org. Lett.* **2006**, *8*, 1987−1990.

(30) Molard, Y.; Bassani, D. M.; Desvergne, J.-P.; Moran, N.; Tucker, J. H. R. *J. Org. Chem.* **2006**, *71*, 8523−8531.

(31) The kinetic data, collected in Table 1, were fitted to a one- or two-exponential decay. A = pre-exponential factor, τ = fluorescence lifetime, k_{exc} = excimer formation rate constant. The goodness of the fits is judged by the χ^2 values and the residual distribution.

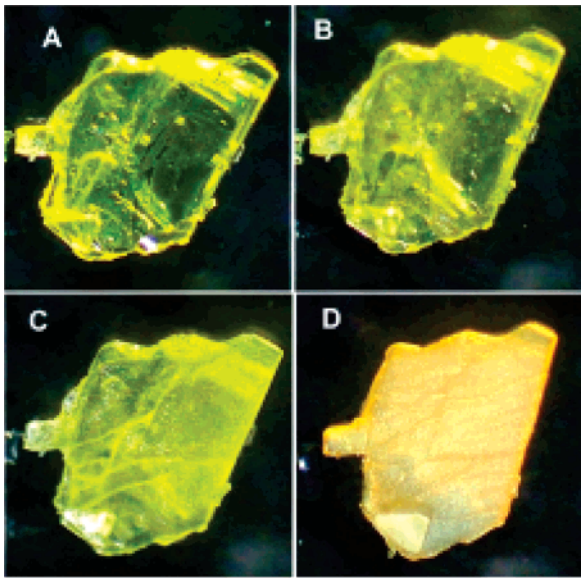

FIGURE 3. Photographs of a 1 mM crystal of monomer **3a** irradiated at visible wavelengths after (a) 0, (b) 1, (c) 16, and (d) 64 h.

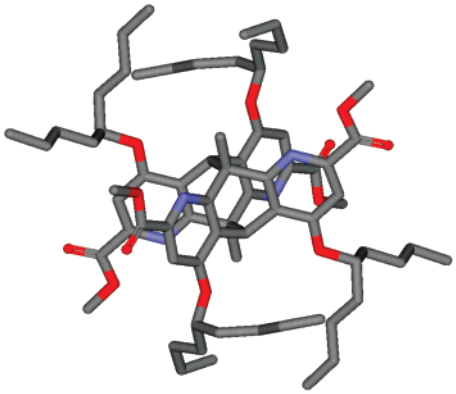

FIGURE 4. Solid-state structure of **11** obtained by irradiation of **3a** at visible wavelengths. Hydrogen atoms have been omitted for clarity.

powder pattern indicating that the crystal had fragmented in the process. Attempts to optimize the conditions to perform a crystal-to-crystal transformation, for example upon irradiating selectively at high wavelengths in the tail of the absorption spectrum, were not undertaken. The product of the irradiation was unambiguously identified as the HT dimer **11** by X-ray crystallography after recrystallization (Figure 4 and Scheme 5). Consistently, NMR ROESY experiments show a strong correlation between the CH_3 protons in position 9 and the proton in position 10.

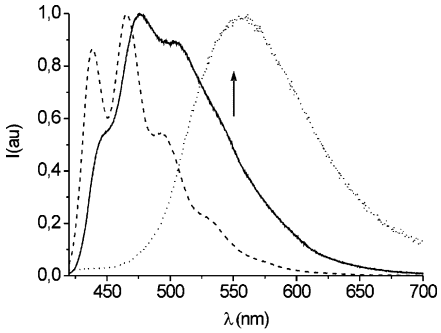

FIGURE 5. Spectrofluorimetric spectra of monomer **3a** (dashed line) and pentamer **6** (bold line) at 2×10^{-5} M in CH_2Cl_2 under anaerobic conditions and of **3a** in the solid state (dotted line), $\lambda_{ex} = 370$ nm.

As judged from NMR spectra, this solid-state photochemical transformation is essentially quantitative. Similar reactions were not attempted with **2** and **4a** because of the difficulty to grow crystals and because of their fragility. Moreover, the highly regular arrangement of the structure of **4a** allows us to speculate that solid-state photodimerization might not be quantitative in this case because HT pairs are not individualized. Two equivalent nearest neighbors exist, allowing each unit to react with the one above or the one below with equal probability, and eventually leaving lonely units unable to react.

The photodimerization of **3a** can also be performed in solution. However, under aerobic conditions, the major product is not the photodimer but the photo-oxide **12** (Scheme 5), the structure of which was assigned based on NMR and mass spectrometry. It is noteworthy that, unlike in solution, the solid-state photodimerization of **3a** does not require protection from oxygen.

Encouraged by these results, we explored the possibility to achieve intramolecular photodimerization between the two terminal diaza-anthracene units of pentamer **6** and transform a helically folded molecule into a covalently locked helix. Since efficient intramolecular photodimerization relies on the proximity between the two anthracene moieties, we first assessed whether the overlap observed in the solid state also prevails in solution using spectrofluorimetry. A comparison between the fluorescence emission spectra of monomer **3a** and of pentamer **6** in solution reveals that the emission of **6** is broadened and shifted bathochromically which suggests the formation of an intramolecular excimer and thus a large overlap between the anthracene moieties (Figure 5). To further investigate this point,

SCHEME 5. Photodimerization and Photooxydation of Monomer 3a

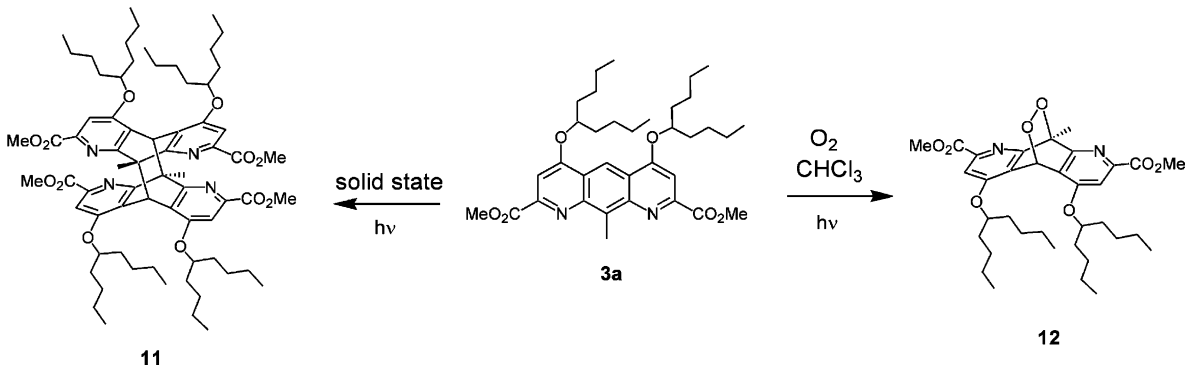

TABLE 1. Kinetic Parameters (τ)[31] of Monomer 3a and Pentamer 6[a]

compound	A_1	τ_1(ns)	A_2	τ_2 (ns)	χ^2	k_{exc} (s^{-1})
3a	1.00	13.98			1.236	
6	0.419	5.46	0.285	35.54	1.048	1.11 10^8

[a] Obtained from fluorescence emission decay at λ_{exc} = 370 nm, at 25 °C in degassed CH_2Cl_2.

fluorescence excited-state lifetime measurements were performed on **6**. The presence of a second decay component in the excited singlet-state lifetimes (Table 1) corroborates the existence of an emissive excimer in solution and a rate constant for its formation can be deduced from the reduction in the lifetime attributed to the locally excited diaza-anthracene singlet excited state.

Since the excimer is a proven intermediate during anthracene photodimerization,[27b] we went along with irradiation of pentamer **6** at λ = 420 nm in benzene solutions at low concentration, 25 °C, and under anaerobic conditions in order to avoid intermolecular adducts and photo-oxidized side products. Fluorescence and UV−vis spectroscopies were used to monitor the eventual disappearance of the diaza-anthracene absorption band but did not reveal any clear sign of reaction, either intramolecular or intermolecular, under these conditions.

Such behavior contrasts with the very efficient photodimerization of **3a** in the solid state but is consistent with the long excited-state lifetime assigned to the intramolecular excimer (35 ns). A fluorescence emission spectrum of **3a** was measured in the crystal state and revealed exclusive excimer fluorescence that is substantially red-shifted compared to the fluorescence of **6** and that lacks the remaining vibronic structure (Figure 5). This is consistent with the reduced electronic stabilization of the intramolecular excimer of **6** in solution versus the intermolecular excimer of **3a** in the solid state, presumably as a result of steric constraints imposed by the helical and rigid nature of the tether. Indeed, the solid-state crystal structure of pentamer **6** (Figure 6) provides some elements as why intramolecular photodimerization is not observed. The structure shows the expected helical conformation with about 4 units per turn that allows a large overlap between the terminal anthracene moieties, consistent with the excimer observed in solution. The distances between the carbons that should be involved in bond formation are 3.36 Å (C9−C9′) and 3.93 Å (C10−C10′). These values are not incompatible with intramolecular photodimerization. However, the two anthracene units significantly deviate from an optimal parallel orientation. Should dimerization occur, it would generate some strain in the macrocyclic product to change its curvature. Additionally, the orientation of the diaza-anthracenes in the helix could only lead to the formation of a HH dimer, which was never detected in the photodimerization of monomer **3a** in solution. The HH dimer is probably disfavored because of its large dipole moment (steric reasons might not be invoked since 9-methyl anthracene is known to form both HT and HH dimers). In short, we presume that even if intramolecular photodimerization occurs in **6**, the product might have a very low thermal stability and may spontaneously decompose back to the starting material. Further efforts are currently being devoted to the design of helically folded aromatic amides optimized for intramolecular photodimerization.

Aggregation Properties. Aromatic amide foldamers have a preferred planar conformation. If curvature exists within this plane, elongation of the strand eventually causes a steric clash between its extremities and deviation from planarity into a helix. Whether in crescent or in helical conformations, a large planar or almost planar aromatic surface is exposed and available for extensive intermolecular $\pi-\pi$ interactions. The clearest manifestation of such intermolecular interactions is the formation of double helical hybrids between pyridinecarboxamide oligomers.[11] In these hybrids, each helical strand further deviates from planarity and undergoes a spring-like extension to wind around the other strand. It follows that the intermolecular surface of $\pi-\pi$ interactions is maximal. The enthalpic gain associated with $\pi-\pi$ interactions compensates the enthalpic cost of the strand spring-like extension. In this context, the large aromatic surface of 1,8-diaza-anthracenes was expected to promote aggregation.

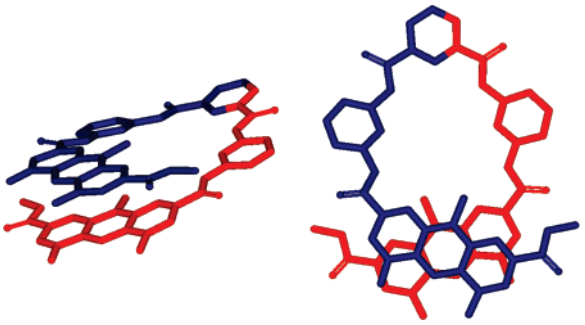

FIGURE 6. Solid-state structure of pentamer **6** crystallized from CH_2Cl_2/hexane. Hydrogen atoms, nonyl side chains and solvent molecules have been omitted for clarity. The asymmetric unit corresponds to half a molecule.

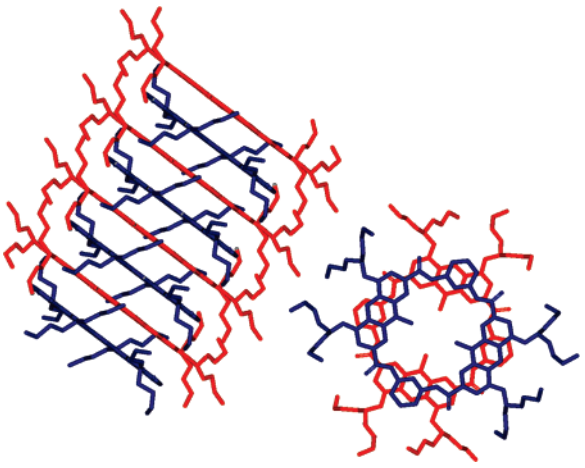

FIGURE 7. Side view and top view and the columnar stack formed by macrocycle **7** in the solid state. Hydrogen atoms have been omitted for clarity. The top view illustrates that consecutive macrocycles in a stack, in red and blue, respectively, are rotated by 90° from one another.

The large aromatic surface provided by 1,8-diaza-anthracene monomers for $\pi-\pi$ interactions is obvious in the crystal structure of macrocycle **7** (Figure 7). In the crystal, the macrocycle adopts a rigorously flat conformation with the amide protons pointing inward to the endocyclic nitrogen atoms. The macrocycles pile up at a distance of ca. 3.35−3.39 Å to form columnar stacks. Consecutive macrocycles in the columns are rotated at a 90° angle from each other, so that each pyridine ring stacks over a diaza-anthracene and reciprocally. In solution, ^{1}H NMR spectra of **7** in $CDCl_3$ showed broad signals of the aromatic protons that shift upfield upon increasing concentration, suggesting that π-stacking interactions also occur in solution.

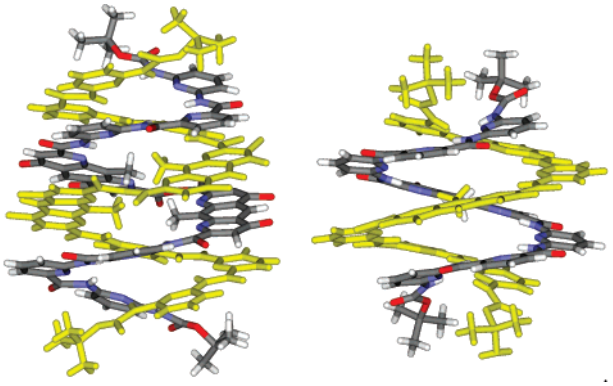

FIGURE 8. Solid-state structures of heptamer **9**[11i] (right) and octamer **10** (left) both crystallized from toluene/hexane. Isobutyl side chains and included solvent molecules have been removed for clarity.

Another aspect of the enhanced aggregation brought by diaza-anthracene units was observed in the hybridization properties of heptamer **9** (Figure 8). As we recently reported,[11i] the ability of **9** to form double helical hybrids is dramatically increased, by at least 5 orders of magnitude, by the presence of one 1,8-diaza-anthracene unit in the center of the sequence, compared to a sequence where the central unit is a pyridine. For example, a dimerization constant $K_{dim} = 6.5\ 10^5$ L·mol^{-1} at 298 K was estimated by fluorescence spectroscopy in pyridine,[11i] a solvent known to strongly weaken hybridization of these oligomers. In comparison, the pyridine oligomer shows no detectable hybridization in this solvent. For heptamer **9**, no dimer to monomer equilibrium was observed in other solvents such as CH_3OH, DMSO, $CHCl_3$ or toluene, suggesting that K_{dim} values are above 10^7 L·mol^{-1} in these solvents, even upon heating. We were able to demonstrate that the enhanced hybridization of **9** does not only originate from an augmented surface involved in intermolecular $\pi-\pi$ stacking but also because the wider helix diameter leads to a lower tilt angle of the helical strand with respect to the helix axis, which results in smaller dihedral angles at the arylamide linkages and thus a considerably lowered enthalpic cost of the spring-like extension of the strands during the hybridization process.[11i]

We investigated the behavior of anhydride octamer **10** and found several features suggesting that its propensity to form double helical hybrids is comparable to that of **9**. Its crystal structure could be solved despite very low diffraction intensity and decomposition of the crystals. The crystal structure is of poor quality but clearly reveals a duplex structure in which two strands wind around one another to span over two helical turns (Figure 8). The duplex possesses an overall symmetrical structure: the two strands and also the two extremities of each strand are identical. The aspect of the duplex, and in particular its wide diameter imparted by the diaza-anthracene units are similar to the duplex formed by heptamer **9**.[11i] The wide diameter results in a lower tilt angle of the strands with respect to the helix axis (on average 30°) than in duplexes based on pyridinecarboxamide strands (43°).[11]

The NMR spectra of octamer **10** in $CDCl_3$ also compare well with those of **9** and suggest a very stable double helix in solution (Figure 9). Aromatic signals are all strongly shifted upfield suggesting extensive ring current effects between stacked aromatic rings. For example, signals of the pyridine rings, an electron-poor aromatic, are found between 6 and 7 ppm, and signals belonging to the diaza-anthracene units are found 1 ppm

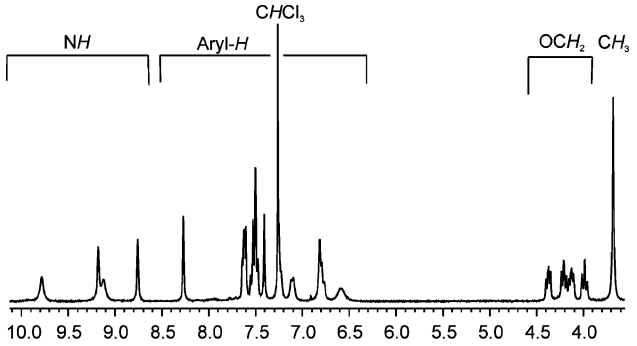

FIGURE 9. Part of the 400 MHz ^{1}H NMR spectra of octamer **10** in $CDCl_3$ at $C = 5$ mM.

upfield in **10** compared with monomer **4b**. As an indication of the intrinsic chirality of a helical structure, the CH_2 and CH_3 groups of the isobutyl side chains of **10** show diastereotopic signals. For example, each of the four methylene protons of a given diaza-anthracene unit of **10** appears as a distinct doublet of doublet (Figure 9). The fact that only one set of signals is observed and that chemical shift values do not change upon diluting a sample from 10 to 0.2 mM suggest that the double helix observed in the crystal also prevails in solution and shows a stability too high to be assessed by ^{1}H NMR ($K_{dim} > 10^6$ mol·L^{-1}). These results thus corroborate those previously obtained with **9**: increasing helix diameter results in a strongly enhanced stability of double helical duplexes in aromatic amide oligomers.

In conclusion, we have prepared several 1,8-diaza-anthracene dicarboxylic acid building blocks and have incorporated them in various cyclic, single helical, and double helical aromatic amide oligomers. These units give rise to anthracene-like photophysical and photochemical behaviors. For example, an emissive excimer was characterized in a single helical oligomer in which two diaza-anthracene units are stacked. These units also result in a strong tendancy of oligomers to engage in intermolecular $\pi-\pi$ interactions either in discrete objects as double helical dimers or in aggregates as columnar stacks. Our studies further enrich the registry of aromatic units to be incorporated in aromatic amide oligomers. Expanding this registry is critical to the scope of structures and functions that may be targetted, because unlike in peptides, aromatic carboxamide oligomer properties depend not only upon the nature of the side chains that they carry but also upon the nature of the main chain. Future developments using diaza-anthracene building blocks include the optimization of intramolecular photochemical cycloadditions in folded helical oligomers.[25]

Experimental Section

Monomer 2. Under an anhydrous atmosphere and protection from light, 2.1 g of compound **1**[22] (6.76 mmol) and 2.2 g of K_2CO_3 (18.6 mmol) were mixed in 30 mL of DMF and heated to 60 °C. Then 1.2 mL of methyl iodide was added, and the mixture was maintained at 60 °C overnight. Then it was poured into 160 mL of water, and the resulting precipitate was filtered and applied to a silica gel column eluting with dichloromethane to give 1.1 g of a yellow solid (44%). ^{1}H NMR ($CDCl_3$, 400 MHz): δ 9.00 (s, 1H), 7.51 (s, 2H), 4.19 (s, 6H), 4.10 (s, 6H), 3.49 (s, 3H). ^{13}C NMR ($CDCl_3$, 100 MHz): δ 166.4, 164.0, 149.7, 145.8, 139.3, 121.4, 113.4, 98.3, 56.3, 53.2, 29.7, 13.1. Crystal structure: see Supporting Information.

Monomer 3a. Under an anhydrous atmosphere and protection from light, compound **1**[22] (2 g, 5.8 mmol) and triphenylphosphine

(3.8 g, 14.6 mmol) were dissolved in anhydrous THF (30 mL) and cooled at 0 °C. 5-Nonyl alcohol (2.6 mL) and diisopropylazadicarboxylate (2.8 mL, 14.6 mmol) were added dropwise at 0 °C. The reaction mixture was stirred for 1 h at 0 °C and then 12 h at room temperature. The solvent was removed by evaporation, and the residue was purified by flash chromatography on silica gel eluting with toluene/ethyl acetate from 8:92 to 10:90 v/v to obtain 3.3 g (90%) of a yellow product. ^{1}H NMR ($CDCl_3$, 400 MHz): δ 9.08 (s, 1H), 7.48 (s, 2H), 4.74 (q, 2H, J = 4.1 Hz), 4.10 (s, 6H), 3.49 (s, 3H), 2.00−1.80 (m, 8H), 1.60−1.20 (m, 16H), 1.00−0.80 (t, 12H, J = 7.2 Hz). ^{13}C NMR ($CDCl_3$, 100 MHz): δ 167.0, 163.4, 150.1, 146.6, 139.4, 122.5, 114.2, 99.5, 79.8, 53.6, 33.5, 27.8, 23.1, 14.4, 13.5. SM (ES): m/z = 594.6 $[M + H]^+$. Crystal structure: see Supporting Information.

Monomer 3b. Under protection from light, monomer **3** (200 mg, 0.34 mmol) was dissolved in 1,4-dioxane/water (50 mL, 8:2 v/v). Sodium hydroxide (34 mg, 0.85 mmol) was added at room temperature. The reaction is carried out till complete disappearance of the starting material, as monitored by thin layer chromatography. Then, acetic acid was added until pH dropped below 7. Dioxane was evaporated and the aqueous solution was washed with CH_2Cl_2. The organic phase was dried with $MgSO_4$ and evaporated to obtain 180 mg (100%) of a yellow solid, which was used without further purification. ^{1}H NMR ($CDCl_3$, 400 MHz): δ 9.16 (s, 1H), 7.69 (s, 2H), 4.54 (q, 4H, J = 5.6 Hz), 3.30 (s, 3H), 2.00−1.80 (m, 8H), 1.60−1.20 (m, 16H), 1.00−0.80 (t, 6H, J = 7.2 Hz).

Monomer 3d. Under protection from light, monomer **3a** (1 g, 1.68 mmol) was dissolved in 1,4-dioxane/water (50 mL, 8:2 v/v) and cooled at 0 °C. Sodium hydroxide (67 mg, 1.68 mmol) was added and the reaction was carried out 2h at 0 °C. Acetic acid was added until pH dropped below 7. The solvent was removed by evaporation and the residue was purified by flash chromatography on silica gel eluting with chloroform/methanol/acetic acid from 99:1:0 to 94:5:1 v/v/v to obtain 510 mg (50%) of a yellow solid. ^{1}H NMR ($CDCl_3$, 400 MHz): δ 9.12 (s, 1H), 7.57 (s, 1H), 7.51 (s, 1H), 4.81 (q, 1H, J = 5.6 Hz), 4.75 (q, 1H, J = 5.6 Hz), 4.10 (s, 3H), 3.41 (s, 3H), 2.00−1.80 (m, 8H), 1.60−1.20 (m, 16H), 1.00−0.80 (t, 12H, J = 7.2 Hz).

Pentamer 6. Under an anhydrous atmosphere and protection from light, compound **3d** (86 mg, 0.15mmol) was activated with $SOCl_2$ (540 μL, 7.5 mmol) at reflux. The reaction was carried out for 20 min, and then $SOCl_2$ was evaporated under vacuum to obtain the monomer **3e**, which was used without further purification. Under an anhydrous atmosphere and protection from light, a solution trimer **5**[15a] (34 mg, 0.067 mmol) and anhydrous triethylamine (28 μL, 0.20 mmol) in anhydrous THF (2 mL) was added to the freshly prepared **3c**, suspended in anhydrous THF (1 mL) at 0 °C. The reaction was stirred at 0 °C for 30 min and then at room temperature for 16 h. THF was removed, and the solid was washed in CH_2Cl_2/H_2O. The organic phase was dried over $MgSO_4$, filtered, and evaporated. The solid residue was purified by flash chromatography on silica gel eluting with chloroform/methanol 99.5:0.5 v/v to obtain 15 mg (16%) of a yellow solid. ^{1}H NMR ($CDCl_3$, 400 MHz): δ 10.56 (s, 1H), 9.10 (s, 1H), 7.81 (d, 1H, J = 7.8 Hz), 7.71 (s, 1H), 7.55 (t, 1H, J = 7.8 Hz), 7.49 (s, 1H), 6.33 (d, 1H, J = 7.8 Hz), 4.81 (q, 1H, J = 5.8 Hz), 4.75 (q, 1H, J = 5.8 Hz), 4.11 (s, 3H), 3,52 (s, 3H), 2.00−1.80 (m, 8H), 1.60−1.20 (m, 16H), 1.00−0.80 (t, 12H, J = 7.2 Hz). ^{13}C NMR ($CDCl_3$, 100 MHz): δ 166.5, 162.9, 162.5, 162.4, 161.6, 150.4, 149.6, 149.1, 148.7, 145.2, 144.0, 140.4, 138.7, 137.1, 125.7, 121.1, 121.0, 113.0, 110.4, 109.5, 98.6, 96.3, 79.3, 79.1, 53.0, 33.0, 32.6, 27.3, 27.1, 22.6, 14.0. Crystal structure: see Supporting Information.

Macrocycle 7. Under an anhydrous atmosphere and protection from light, compound **3b** (100 mg, 0.18 mmol) was activated with $SOCl_2$ (1.3 mL, 1.76 mmol) at reflux. The reaction was carried out for 1 h, and then $SOCl_2$ was evaporated under vacuum to obtain monomer **3c**, which was used without further purification. Under an anhydrous atmosphere and protection from light, a solution of 2,6-diaminopyridine (20 mg, 0.18 mmol) and anhydrous *N*,*N*-diisopropylethylamine (77 μL, 0.44 mmol) in anhydrous THF (2 mL) was added to the freshly prepared **3c**, suspended in anhydrous THF (1 mL) at 0 °C. The reaction was stirred at 0 °C for 30 min and then at room temperature for 16 h. The THF was removed, and the solid was washed in CH_2Cl_2/H_2O. The organic phase was dried over $MgSO_4$ and evaporated. The solid residue was purified by flash chromatography on silica gel eluting with chloroform to obtain 50 mg (50%) of a yellow solid. ^{1}H NMR ($CDCl_3$, 400 MHz): δ 10.65 (broad s, 4H), 8.67 (broad s, 2H), 7.49 (broad s, 2H), 7.37 (m, 6H), 4.88 (broad t, 4H), 3.96 (broad s, 6H), 2.20−0.80 (m, 76H). ^{13}C NMR ($CDCl_3$, 100 MHz): δ 164.1, 161.7, 150.5, 148.5, 145.0, 139.6, 136.6, 121.9, 114.9, 107.4, 96.4, 79.6, 33.3, 30.0, 27.7, 23.2, 14.4. SM (Maldi-TOF): m/z = 1279,70 $[M + H]^+$. Crystal structure: see Supporting Information.

Compound 11. Crystals of monomer **3a** obtained in CH_2Cl_2/heptane were irradiated for 72 h with a visible wavelength lamp in a quartz cell at 20 °C. The HT photoadduct **11** was obtained quantitatively. ^{1}H NMR ($CDCl_3$, 400 MHz): δ 7.07 (s, 4H), 5.08 (s, 2H), 4.22 (q, 4H, J = 5.4 Hz), 3.87 (s, 12H), 2.40 (s, 3H), 1.80−1.20 (m, 48H), 1.01 (t, 12H, J = 7.2 Hz), 0.84 (t, 12H, J = 7.2 Hz,). Crystal structure: see Supporting Information.

Compound 12. A concentrated solution (50 mM) of monomer **3a** in $CHCl_3$ was irradiated for 4 h with a visible wavelength lamp in a quartz cell at 20 °C. The reaction mixture was purified by chromatography on silica gel eluting with toluene/ethyl acetate 4:98 v/v to obtain the photo-oxidized product **12**. ^{1}H NMR ($CDCl_3$, 400 MHz): δ 7.60 (s, 2H), 6.86 (s, 1H), 4.52 (q, 2H, J = 5.8 Hz), 3.97 (s, 6H), 2.33 (s, 3H), 1.80−1.20 (m, 24H), 0.93 (t, 6H, J = 7.2 Hz), 0.84 (m, 12H). HRMS: calcd $[M + H]^+$ ($C_{35}H_{51}N_2O_8$) 627.3645, found (ESI) 627.3643.

Octamer 10. Octamer **10** was obtained as side product in 4% yield during the already described synthesis of heptamer **9**.[11i] ^{1}H NMR ($CDCl_3$, 400 MHz): δ 9.74 (s, 2H), 9.19 (2s, 4H), 8.78 (s, 2H), 8.28 (s, 2H), 7.61 (m, 4H), 7.48 (m, 6H), 7.41 (s, 2H), 7.21 (d, 1H), 7.10 (d, 1H), 6.80 (m, 3H), 6.60 (d, 1H), 4.37 (t, 2H), 4.20 (t, 2H, J), 4.11 (t, 2H), 3.98 (t, 2H), 3.67 (s, 6H,), 2.58 (m, 2H), 2.47 (m, 2H), 1.43 (m, 24H), 0.43 (s, 18H). ^{13}C NMR ($CDCl_3$, 100 MHz): δ 162.3, 162.2, 160.5, 160.2, 159.4, 158.9, 152.2, 151.0, 149.4, 148.5, 148.3, 147.9, 147.8, 146.7, 146.2, 144.7, 143.3, 139.9, 139.7, 138.4, 137.7, 124.2, 123.5, 120.4, 120.2, 113.3, 109.4, 108.7, 108.1, 107.1, 98.5, 95.8, 75.1, 75.0, 28.5, 27.0, 19.4, 19.3, 19.1, 13.8. SM (ES): m/z = 1697.8 $[M + H]^+$. Crystal structure: see Supporting Information.

Crystallography. Data were collected using three types of diffractometers: a sealed tube generator with graphite monochromatized Cu Kα radiation and a single point detector (**3a**, **11**); a sealed tube generator with graphite monochromatized Mo Kα radiation and a CCD camera (**2**, **4a**); a micofocus rotating anode generator with monochromatized Cu Kα or Mo Kα radiation with an image plate detector (**6**, **7**, **10**). The positions of non-H atoms were determined by the program SHELXS 87, and the position of the H atoms were deduced from coordinates of the non-H atoms and confirmed by Fourier Synthesis. H atoms were included for structure factor calculations but not refined. Crystallographic parameters are reported in the Supporting Information.

Acknowledgment. This work was supported by the CNRS (predoctoral fellowship to C.D. and postdoctoral fellowship to C.Z.) and by an ANR grant (project No. NT05−3_44880). We thank Dr. Dario M. Bassani and Dr. Nathan McClenaghan, Institut des Sciences Moléculaires, Université Bordeaux 1−CNRS, for assistance with spectrofluorimetric measurements and interpretation.

Supporting Information Available: General Experimental Methods. NMR spectra of products **2** to **12**. This material is available free of charge via the Internet at http://pubs.acs.org.

JO702602W